Table 1 Combined effects of thrust slope and thrust level at $M=3.0$

Thrust slope	Thrust-to-drag ratio	Phugoid damping ratio	Height-mode root
a	1	−0.04[a]	0.04[a]
b	1	0.01	−0.005
a	4	−0.27[a]	0.02[a]
b	4	−0.16[a]	−0.02

[a]Unstable.

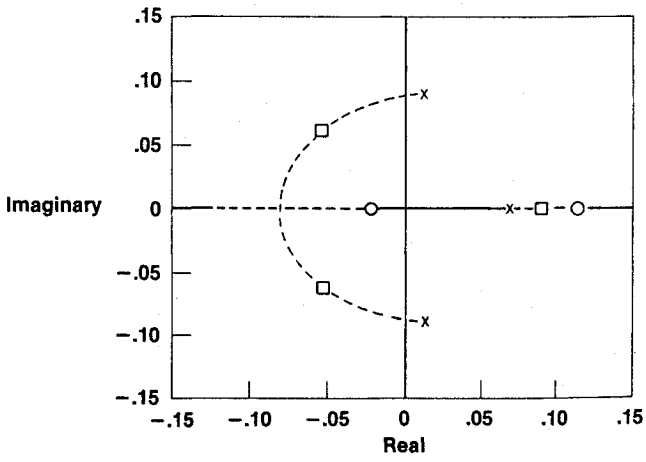

Fig. 3 Root locus of advanced air breather with pitch attitude feedback (long period).

2). As noted by Stengel, positive thrust slopes were destabilizing to both the phugoid and height mode.[3] On the other hand, thrust level primarily influenced phugoid damping. Increases in thrust-to-drag ratio were destabilizing and these effects were not grossly affected by Mach number. Consequently, the most critical combination of thrust slope and thrust level occurred at $M=3.0$. A summary of $M=3.0$ results is presented in Table 1.

Note that thrust slope *b* equals zero and corresponds to a simple air breather. It can be seen that the advanced air breather (thrust slope *a*) has more unstable long-period modes than the simple air breather (thrust slope *b*) at low and high thrust-to-drag ratios (1 and 4). Increasing the thrust-to-drag ratio significantly destabilizes the phugoid, resulting in a much more negative damping ratio for both thrust slope cases. Increasing the thrust level stabilizes the height mode. However, for thrust slope *a*, the height mode is still unstable, whereas for thrust slope *b*, a nearly neutral mode becomes significantly stable. The difference between a simple air breather (*b*) with no thrust level effects ($T/D=1$) and an advanced air breather (*a*) at a $T/D=4$ is especially noteworthy. It can be seen that the former has a slightly stable phugoid damping ratio of 0.01 and a slightly stable height-mode root of −0.005. The latter (advanced air breather) has a significantly unstable phugoid damping ratio of −0.27 and a significantly unstable height-mode root of 0.02. This illustrates the strong influence the propulsion system can have on the long-period dynamics.

Basic Feedback Control

Pitch attitude feedback to the pitch control surface is a common means of improving phugoid damping of conventional aircraft. Even at high speeds, in the absence of propulsion system effects, aircraft tend to be relatively conventional since the height mode has a pole and zero near the origin that tend to cancel each other. An advanced air breather, however, has a height-mode pole and zero in the right-half plane, and attempts to improve phugoid damping with attitude feedback make the height mode more unstable. This is illustrated in Fig. 3. However, as shown by Stengel and others, velocity and altitude feedback loops can be used to alter the phugoid and height-mode characteristics.[3] This avoids the problems presented by the use of attitude feedback.

Concluding Remarks

The propulsion system is a dominant influence on the stability of aerospace vehicle longitudinal long-period modes. These effects are most significant in the $M=3.0$ range caused by the large changes in thrust with Mach number associated with engine cycle changes. The modes cannot be simultaneously stabilized with pitch attitude feedback but can be stabilized with velocity and attitude feedback loops.

References

[1]Etkin, B., "Longitudinal Dynamics of a Lifting Vehicle in Orbital Flight," Inst. of Aeronautical Sciences National Summer Meeting, Los Angeles, CA, June 28-July 1, 1960, IAS Paper 60-82.

[2]Porter, R. F., "The Linearized Long-Period Longitudinal Modes of Aerospace Vehicles in Equilibrium Flight," AFFTC-TN-61-2, 1961.

[3]Stengel, R. F., "Altitude Stability in Supersonic Cruising Flight," *Journal of Aircraft*, Vol. 7, No. 5, 1970.

Stability Tests of Spin-Stabilized Spacecraft in the Presence of Thrust

Rudolf X. Meyer*
The Aerospace Corporation,
Los Angeles, California 90009

Nomenclature

a_s	= space vehicle acceleration
Fr	= Froude number [Eq. (4)]
$I_x = I_y, I_z$	= moments of inertia
ℓ_s, ℓ_m	= characteristic lengths of spacecraft and model, respectively
m_s	= spacecraft mass
n	= z component of angular velocity
R	= center-of-mass radial position (Fig. 1)
r	= sensor array radial position (Fig. 1)
s	= vertical distance from center of mass to sensor array (Fig. 1)
T	= thrust
(X,Y,Z)	= laboratory (inertial) reference frame
(X',Y',Z')	= nonrotating frame attached to center of mass (accelerating)
(x,y,z)	= body-fixed frame
θ	= nutation angle
λ	= precession rate
ξ,η	= coordinates defining excursion of light beam from array center
σ	= inertia ratio
ψ	= turntable position
ω_{xy}	= transverse angular velocity

Subscripts

0	= mass center
m	= model
s	= spacecraft

Received April 24, 1989; revision received June 15, 1989.

*Consultant; also, Adjunct Professor, Department of Mechanical, Aerospace, and Nuclear Engineering, University of California, Los Angeles. Fellow AIAA.

Introduction

SPECIAL considerations apply when examining the stability of spin-stabilized spacecraft to which thrust is applied, such as during the firing of perigee or apogee rocket motors. A disturbing torque, produced by the thrust force, will arise, for instance, when spacecraft propellant is displaced from its nominal position inside the tanks ("propellant sloshing").

More recently, an instability evidenced by a growing nutation angle has been observed during the upper-stage firing of certain solid-propellant rocket motors. This instability has been variously ascribed to gasdynamic effects,[1,2] or to the sloshing of a pool of liquid slag accumulated in the aft section of the motor. A theoretical analysis, representing the fluid (propellant or slag) by a displaced mass point, has been developed by Mingori and Yam.[3] Liquid sloshing and its effect on spacecraft have been partially tested in several laboratories. In these tests, true thrust is absent, but on the other hand, the spacecraft—which is supported at its center of mass but is otherwise free to rotate—is subject to the gravity-reacting force at its support. Test models are spinning and precessing, and, in some cases, free to nutate.

It is well recognized, however, that the gravitational support force present in laboratory tests, even if it could be scaled to the actual magnitude of the thrust, cannot properly simulate the latter. As the spacecraft nutates, the thrust remains aligned with the vehicle axis. Hence, the thrust is of the type referred to in mechanics as a "follower force," whereas the gravitational force acting on the test article is stationary. For this reason, it has generally been assumed, incorrectly as it turns out, that an exact laboratory simulation of a thrusting spacecraft with liquid stores was impossible.

This Note describes the design of a test rig that satisfies the simulation of the thrust as a follower force. This is accomplished by means of a turntable on which the spacecraft model is mounted eccentrically. Briefly discussed also are the scaling laws that relate the spacecraft to the test article.

Test Rig Design

The spacecraft model is supported at its nominal center of mass by a spherical airbearing (AB), which allows spin, precession, and nutation of the model (Fig. 1). If the airbearing's position is fixed in the laboratory frame of reference, the follower force cannot be simulated. Contrasting with this, and as will be described, the airbearing is accelerated in such a way that the resultant of the gravity and inertial forces remains aligned at all times with the thrust vector.

To achieve this, the airbearing rests eccentrically on a horizontal turntable (TT), rotated by motor M-3. The variable eccentricity R of the airbearing—hence, of the spacecraft model—is determined by the rotation of the threaded shaft driven by motor M-2. Through an electric network discussed later, M-2 is slaved to the radial displacement r of the center of a photoelectric sensor array (PA), the position of which is determined by the rotation of motor M-1. An optical system, mounted on the spacecraft model, provides a light beam (LB) that illuminates the photoelectric array. The array is made to follow the instantaneous position of the light beam, the radial position of the array being determined by M-1 and M-2, and its azimuthal position by M-3.

In testing the stability of spacecraft that contain liquid stores, the perturbing moments are typically small so that the time constants for damping or unstable growth are long compared with the precession time. Hence, one can describe the motion at each instant as approximately a free precession with a slowly decreasing or increasing nutation angle (designated in Fig. 1 by θ_m).

If we assume an inertially symmetric spacecraft with equal transverse principal moments of inertia I_x and I_y about the center of mass, it follows that the transverse component ω_{xy} of the instantaneous angular velocity rotates relative to the body-fixed axes x,y,z with angular velocity $\lambda=(\sigma-1)n$ in the transverse plane.[4] Here, σ is the moment-of-inertia ratio $I_z/I_x=I_z/I_y$, and n the z component of the angular velocity (n is strictly constant if the perturbing torque has no z component). The nutation angle θ is given by $\tan\theta=\omega_{xy}/(\sigma n)$.

We require that the model—which does not need to be full scale—have the same inertia ratio as the spacecraft; hence, $\sigma_m=\sigma_s$. (An additional restriction on the modeling is discussed

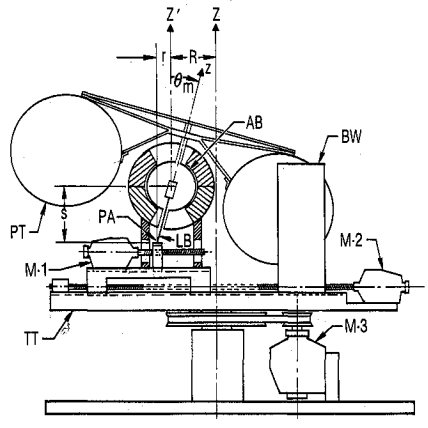

Fig. 1 Schematic of test rig. PT: spacecraft propellant tanks; BW: balance weights. Other symbols are explained in the text. Not shown is the apparatus needed for spin-up and for initial setting of the nutation angle of the test article.

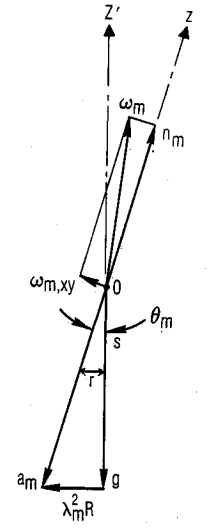

Fig. 2 Diagram illustrating Eqs. (2) and (3), for the free precession of a model of a prolate ($\sigma<1$) spacecraft; ω_m: model angular velocity; n_m and $\omega_{m,xy}$: axial and transverse components of ω_m; 0: center of mass. Other symbols are explained in the text.

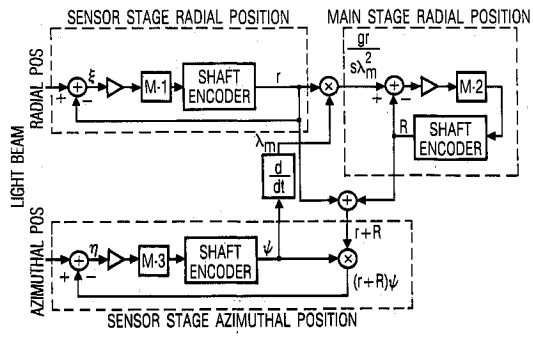

Fig. 3 Electrical network for the control of motors M-1, M-2, and M-3.

in the next section.) We have, therefore, the relation

$$\lambda_m/\lambda_s = n_m/n_s \tag{1}$$

The test is started at some chosen value $\theta_m(0)$, with the angular momentum vector vertical and the turntable rotating at the angular velocity λ_m. If the horizontal Cartesian coordinates of the center of mass are designated by $X_0(t)$, $Y_0(t)$, in the laboratory (inertial) frame, it follows that

$$X_0 = -R\cos(\lambda_m t), \qquad Y_0 = -R\sin(\lambda_m t)$$

Hence, the center of mass of the model is accelerated in the horizontal plane by the amounts

$$\ddot{X}_0 = \lambda_m^2 R\cos(\lambda_m t), \qquad \ddot{Y}_0 = \lambda_m^2 R\sin(\lambda_m t)$$

The corresponding force that will appear in a nonrotating reference frame (X',Y',Z') that moves with the center of mass, when combined with the gravitational force, leads to the requirement (Fig. 2)

$$\lambda_m^2 R/g = \tan\theta_m \tag{2}$$

where g is the gravitational acceleration, in order that the vector sum of the forces will be aligned at all times with the model's z axis.

If s is the vertical distance from the center of mass to the horizontal plane of the sensor array (Fig. 1), and r the excursion from the array's null position at $X' = Y' = 0$, then $\tan\theta_m = r/s$. Hence, for the force acting on fluids such as propellants or slag to be a proper follower force and to be proportional to the thrust, we need to require that

$$R = (g/s\lambda_m^2)r \tag{3}$$

A closed-loop electrical network to control R according to this relationship and to control the rotation angle ψ of the turntable is indicated in Fig. 3. Error signals ξ and η are generated by opposing pairs of photoelectric elements when the light beam is not centered on the array (Fig. 1). The quantities $gr/(s\lambda_m^2)$ and $(r+R)\psi$ are generated by the network and control the motors M-2 and M-3 (Fig. 3).

Spacecraft/Model Similarity Relation

The test article is required to be a scale model of the spacecraft, with identical inertia ratios σ and initial nutation angle $\theta(0)$. To simulate the dynamics of fluid sloshing, it is also required that the Froude numbers Fr_m of the model and Fr_s of the spacecraft

$$Fr_m = n_m^2 \ell_m/a_m, \qquad Fr_s = n_s^2 \ell_s/a_s \tag{4}$$

be the same, where a_m and a_s are the acceleration terms parallel to the z axis. For the model, $a_m = g/\cos\theta_m$; for the spacecraft, $a_s = T/m_s$. It follows that the z component n_m of the model's angular velocity must be chosen according to the rule

$$n_m = n_s\sqrt{\ell_s g m_s/\ell_m T\cos\theta(0)} \tag{5}$$

Thus, for instance, for a spacecraft with $n_s = 6.28\ \text{s}^{-1}$ (corresponding to 60 rpm), $\sigma = 0.50$ (hence, a prolate configuration), $T/m_s = 4.0\ g$, $\ell_s/\ell_m = 2.00$, and $\theta(0) = 10.0$ deg, similarity requires $n_m = 4.47\ \text{s}^{-1}$ (corresponding to 42.7 rpm); hence, $\lambda_m = -2.24\ \text{s}^{-1}$. For a test rig design with $s = 20$ cm, it follows that $r = 3.53$ cm, and from Eq. (3), $R = 34.5$ cm.

Conclusion

Contrary to opinions sometimes held, it is possible to design a test rig that is capable of verifying in the laboratory the stability of a space vehicle in the presence of thrust. This is achieved by mounting the scaled or full-scale spacecraft model eccentrically on a rotating platform in such a way that the additional forces introduced in the noninertial reference frame, when added to the laboratory gravity, just provide the lacking (scaled) thrust component.

References

[1]Meyer, R. X., "Convective Instability in Solid Propellant Rocket Motors," *Astrodynamics,* Vol. 54, Advances in the Astronautical Sciences, AAS Paper 83-368, American Astronautical Society, San Diego, CA, 1983.

[2]Flandro, G. A., et al., "Fluid Mechanics of Spinning Rockets," Air Force Rocket Propulsion Lab., Edwards AFB, CA, Rept. TR-86-072, 1986; also, Flandro, G. A., "Interaction of Inertial Waves in a Spinning Propellant Rocket Motor with Spacecraft Motion," Air Force Rocket Propulsion Lab. Rept., 1982.

[3]Mingori, D. L., and Yam, Y., "Nutational Stability of a Spinning Spacecraft with Internal Mass Motion and Axial Thrust," AIAA Paper 86-2271, 1986.

[4]Kaplan, M. H., *Modern Spacecraft Dynamics and Control,* Wiley, New York, 1976, Chap. 2.

Comparison of the Least-Squares Moving-Block Technique with Ibrahim's Method

Ahmed Omar Amrani*
Advanced Rotorcraft Technology, Inc., Mountain View, California 94043

Introduction

MODAL parameters of a given dynamical system can be identified from either the transient time response[1-3] or the forced time response to a control input.[4,5] A new approach for the modal identification from transient time history data is presented here. The method is applied to two test examples to evaluate and compare its performance to the Ibrahim sparse time domain algorithm.

Least-Squares Moving-Block Technique

The theory supporting the least-squares moving-block technique (LSMBT) has already been developed for a single time history[6]; a generalization to any given number of time histories is presented here. Assuming that a number of discretized transient time histories are available from either measurements or computer simulation, the goal is to estimate the modal parameters of the active modes contained in the time history data. Consider a system of p discretized transient signals

$$S_n = \sum_{k=1}^{2m} \eta_k e^{\lambda_k t_n} \qquad t_n = n\Delta t \qquad n = 0,1,2,\ldots \tag{1}$$

$$\lambda_k = -\sigma_k + j2\pi f_k \qquad k = 1,2,3,\ldots,2m \tag{2}$$

$$S_n = \begin{bmatrix} s_{1n} \\ s_{2n} \\ \cdots \\ s_{pn} \end{bmatrix} \qquad \eta = [\eta_1,\eta_2,\ldots,\eta_k,\ldots,\eta_{2m}] \tag{3}$$

Received March 23, 1989; revision received June 16, 1989.

*Aerospace Engineer.